Chapter 1
LPG Sensing Properties of Electrospun In-Situ Polymerized Polyaniline/MWCNT Composite Nanofibers

Pallavi T. Patil, Pravin S. More and Subhash B. Kondawar

Abstract In this paper, we report the fabrication of poly(methyl methacrylate) (PMMA) nanofibers by electrospinning technique and used as substrate for coating pure polyaniline (PANI) and PANI/multiwalled carbon nanotubes (MWCNT) separately during chemical oxidative polymerization. The morphology and structure of PANI and PANI/MWCNT nanofibers were investigated by SEM, UV-VIS, FTIR and XRD. SEM shows that the fibrous structure of PMMA with an average fiber diameter 272 nm. UV-Vis, FTIR and XRD analyses confirmed the formation of PANI and its interaction with MWCNT. Electrical responses of the synthesized samples towards LPG were measured at room temperature for various ppm, which fulfill all the characteristics like sensitivity, response, recovery of the sensors. Sensitivity study shows that materials under investigation are found to be highly sensitive for LPG near to room temperature. PANI/MWCNT nanofibers showed rapid and reversible resistance change upon exposure to LPG as compared to that of PANI nanofibers, which may be due to MWCNT wrapped by conducting PANI results in the formation of a charge transfer complex which increases the protonation of the polyaniline and the transition in the electrical resistance was attributed to a change in the localization length of the composite nanofibers.

1.1 Introduction

In recent years, detection of gases and diagnose their compositions has constantly gaining much more interest and turned into a prime concern for human wellbeing. Liquefied Petroleum Gas (LPG) is highly inflammable gas and common fuel used for domestics, industrial and commercial appliances. Generally, LPG composed of volatile low boiling point gases—*iso*-butane, ethane, propane, *n*-butane, butylene, *iso*-butene, *trans*-2-butene, propene, *cis*-2-butene, *iso*-pentane and *n*-pentane due to

P. T. Patil · S. B. Kondawar (✉)
Department of Physics, Rashtrasant Tukadoji Maharaj Nagpur University, Nagpur, India
e-mail: sbkondawar@yahoo.co.in

P. S. More
Department of Physics, Institute of Science, Mumbai, India

R.-I. Murakami et al. (eds.), *NAC 2019*, Springer Proceedings in Physics 242,
https://doi.org/10.1007/978-981-15-2294-9_1

the availability of higher boiling point components [1–5]. The gas sensing devices based on inorganic materials such as metal oxide semiconductors, which works on principle of the change in conductivity with interaction of gas molecules. However, they generally have a low selectivity to specific target gases and high operation temperature and thus increase power consumption, reduce sensor life, limit the portability, etc. [6]. Therefore, several different approaches have been explored in order to overcome these issues. A new approach is needed to increase this selectivity and sensitivity at room temperature (300 K). The room temperature operation is also an important criterion to achieve intrinsically safe performance in potentially hazardous situations. It has been pointed out that such sensors exhibit a fast, reversible response at room temperature [5, 6]. Conducting polymers, in comparison are another important category of low cost sensing material proven to have high sensitivity, fast response and room temperature operation and the possibility of tuning both chemical and physical properties by using different substituents [7, 8]. Polyaniline, polypyrrole, and polythiophene are most widely studied conducting polymers. Polyaniline is appealing because it is environmentally stable, easily synthesized, and can react with chemical species to behave as protonating or deprotonating agents to change their conductivity at room temperature. The conductivity depends on both the ability to transport charge carriers along the polymer backbone and for the carriers to hop between polymer chains. Any interactions with polyaniline that alters either of these processes will affect the conductivity [8, 9]. Nanocomposites are the combinations of two or more such nanosized objects or nanoparticles synthesized by some suitable techniques shows unique physical properties and wide application potential in diverse areas [10]. Sensing properties are sensitive to materials structure and morphology. In terms of sensitivity, response time, etc., PANI nanofibers were reported to exhibit better sensing properties than thin films because of the high surface-to-volume ratio brought about by the nanostructure [11]. Electrospinning is currently the most promising, relatively easy and fast technique to produce continuous one-dimensional conducting nanofibers on a large scale and the fiber diameter can be adjusted from nanometers to microns [12–14]. Electrospun conducting fibers are stably produced from blend solutions formed by mixing a conducting polymer and a nonconducting polymer, these fibers can have a handicap in terms of their electrical properties compared to pure conducting nanofibers and nanowires fabricated using methods such as electropolymerization and electrodeposition. A good strategy for improving the electrical properties of electrospun conducting fibers is to coat conducting polymer nanocomposites incorporate with MWCNTs on the surface of nonconducting nanofibers, which have superior electrical conductivity, into the conducting polymer [12]. PMMA (polymethylmethacrylate) is a well-known optical wave guiding polymer. PMMA being a pure dielectric has suitable optical properties and PANI can be synthesized to have suitable electrical properties. A composite of PANI/PMMA and PANI/MWCNT/PMMA can be tailored to have the superior synergistic properties of the materials [15].

Carbon nanotubes (CNTs) are an important group of nanomaterials with unique electronic and chemical properties. Since CNTs were discovered in 1991 by Iijima et al., there has been a growing interest among researchers to explore their unique

electrical, physical, mechanical and chemical properties to develop high performance devices in nanotubes for several applications. Researchers have been exploring the potential of Multiwalled carbon nanotubes (MWCNTs) in a wide range of applications: nanoelectronics, sensors, field emission, displays, hydrogen storage, batteries, polymer matrix composites, nanoscale reactors and electrodes. Due to the distortion of the electron clouds of MWCNTs from a uniform distribution in graphite to asymmetric distribution around cylindrical nanotubes, a rich π-electron conjugation forms outside of the MWCNTs, making them electrochemically active. Nanocomposites of a conducting polymer and MWCNTs show synergistic effect and have been made for different applications. MWCNTs have considerable potential in the field of polymer composites. Functionalized nanotubes treated with a mixture of concentrated H_2SO_4:HNO_3 are also more easily dispersed in organic solvents, leading to an improved dispersion and homogeneity of the MWCNTs within the polymer nanocomposite [16, 17]. Studies have revealed that modification of MWCNTs with conducting polymers can significantly enhance their gas sensing properties. Sensing mechanism of MWCNTs based sensor upon exposure to gas molecules mainly depends on the changes in their electrical properties due to charge transfer between MWCNTs and the gas molecules. MWCNT-based sensors are highly advantageous over traditional semiconducting metal oxide based sensors as they offer high conductivities under room temperature and require smaller device architecture. Despite their appealing properties of MWCNTs, poor sensitivity, lack of selectivity, very high recovery time, weak interaction with gas molecules limit their commercial applications. Various attempts have been made to overcome these problems by incorporating functionalized MWCNTs with various conducting polymers to significantly improve their sensor performance [8].

In this paper, poly(methyl methacrylate) (PMMA) nanofibers were prepared by electrospinning technique. On the surface of PMMA nanofibers, PANI was grown by in-Situ polymerization to obtain a composite of coaxial PANI/PMMA (abbreviated as PAPM) and PANI/MWCNT/PMMA (abbreviated as PACPM) nanofibers. The nanostructured composite was successfully studied as gas sensor. Its electrical responses towards LPG were measured at room temperature for various ppm.

1.2 Experimental

1.2.1 Materials/Chemicals

Aniline (99.5%) was procured from E. Merck and distilled under reduced pressure prior to use. MWCNTs from NPL Delhi, Acetone [$(CH_3)_2 \bullet CO = 58.08$] were procured from Fisher Scientific. Poly(methyl methacrylate) (PMMA) [Mol. Wt 3, 50,000] from sigma aldrich, Sulfuric acid, Hydrochloric Acid, Chloroform, Ammonium Persulphate (98%) and *N*,*N*-Dimethylformamide (DMF) were procured from

Merck and used as received. All chemicals were of analytical grade and solutions were prepared with double distilled water.

1.2.2 Synthesis of Poly(Methyl Methacrylate) (PMMA) Nanofibers

Nanofibers of PMMA were prepared by using electrospinning technique [18]. Typically, a solution of PMMA in dimethylformamide (DMF) was filled in a syringe bearing a hyperdermic needle, which was connected with a high-voltage power supply and electrospun at a voltage of 20 kV. An aluminium foil was grounded and worked as the collector. The distance between the needle tip and the grounded collector was 18 cm. The flow rate of the solution was kept at 0.4 mL/h [11, 15]. The electrospun PMMA nanofibers were collected and dried at 80 °C for overnight in vacuum oven.

1.2.3 Fabrication of PAPM and PACPM Nanofibers

In the typical reaction, 0.2M aniline oxidized with aqueous medium of 0.25M ammonium persulfate with dopeant HCl. Dip some amount of as-synthesized PMMA nanofibers into the aniline solution then add ammonium persulfate dropwise in aniline solution, briefly stirred, and left to polymerize at room temperature (~18–24 °C). Next day, the PAPM nanofibers were collected on a filter, washed with three 100-mL portions of 0.2M HCl, and similarly several times with distilled water. PAPM nanofibers were kept in vacuum oven at 60 °C. PANI prepared under these reaction and processing conditions are further referred to as "standard" samples [18–20]. For the synthesis of PACPM nanofibers, same reaction was followed as synthesis of PAPM but this time addition of fixed amount of functionalized MWCNTs with respect to the amount of aniline into the aniline solution was done. Schematic representation of the synthesis of PAPM nanofibers is shown in Fig. 1.1.

1.2.4 Characterizations

Morphological studies of the PMMA, PAPM and PACPM nanofibers were examine by Scanning Electron Microscopy (SEM, Carl Ziess, SEM EVO18). For Spectral analysis FT-IR spectra were obtained on a Thermo Nicolet, Avatar 370 infrared spectrometer from 400 to 4000 cm^{-1}. Spectrophotometric measurements were carried out by PerkinElmer UV/Vis Spectrometer Lambda 35 (in the wavelength range of 200–800 nm). Evaluation of X-ray diffraction (XRD) patterns were done by powder

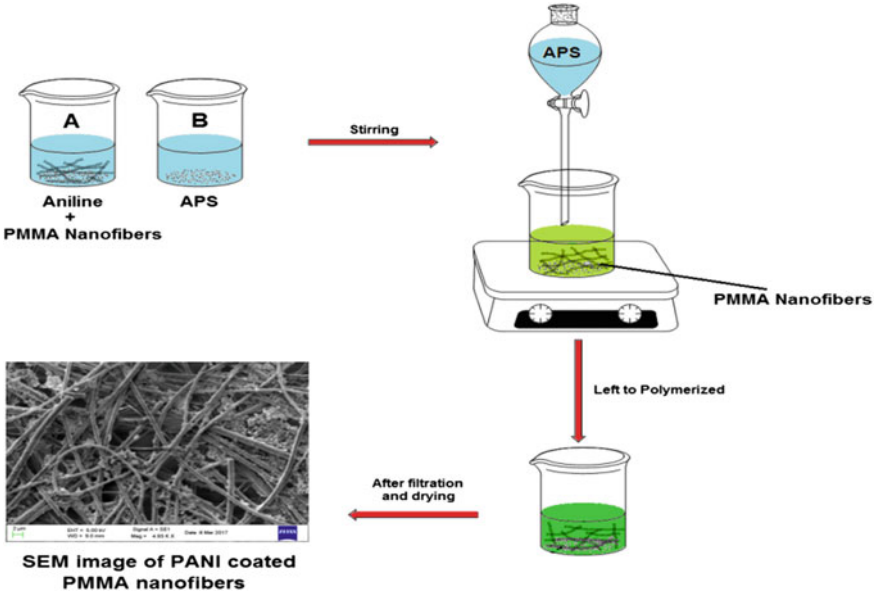

Fig. 1.1 Schematic representation of the synthesis of PAPM nanofibers

X-ray diffraction (Bruker AXS D8 Advance instrument (Cu-Kα, wavelength 1.540 Å and range of $2\theta = 10° - 90°$)).

1.3 Results and Discussions

1.3.1 Scanning Electron Microscopy (SEM)

SEM micrographs of PMMA, PAPM and PACPM nanofibers are presented in Fig. 1.2a–c with their respective histograms respectively. From Fig. 1.2a it can be seen that the nanofibers electrospun from PMMA in DMF solution with a concentration of 0.1 g/mL had a diameter 272 nm. Ji et al. reported that when the concentration of PMMA was increased 0.18–0.32 g/mL, the nanofibers obtained were much thicker, with a diameter up to 900 nm [11]. After the deposition of PANI on PMMA nanofibers by in-Situ polymerization, the diameters of fibers were increased to 502 nm in average. It is clearly seen that the composite nanofibers were quite smooth, with somewhat aggregations of PANI nanoparticles on the surface of PMMA nanofibers. The SEM observation indicates that smooth composite nanofibers have been successfully obtained. Furthermore, it is worth noting that the PAPM nanofibers showed good adherence to the underlying to electrodes, which may lead to a high sensitivity to the analyte. Figure 1.2c is the scanning electron micrograph of PACPM

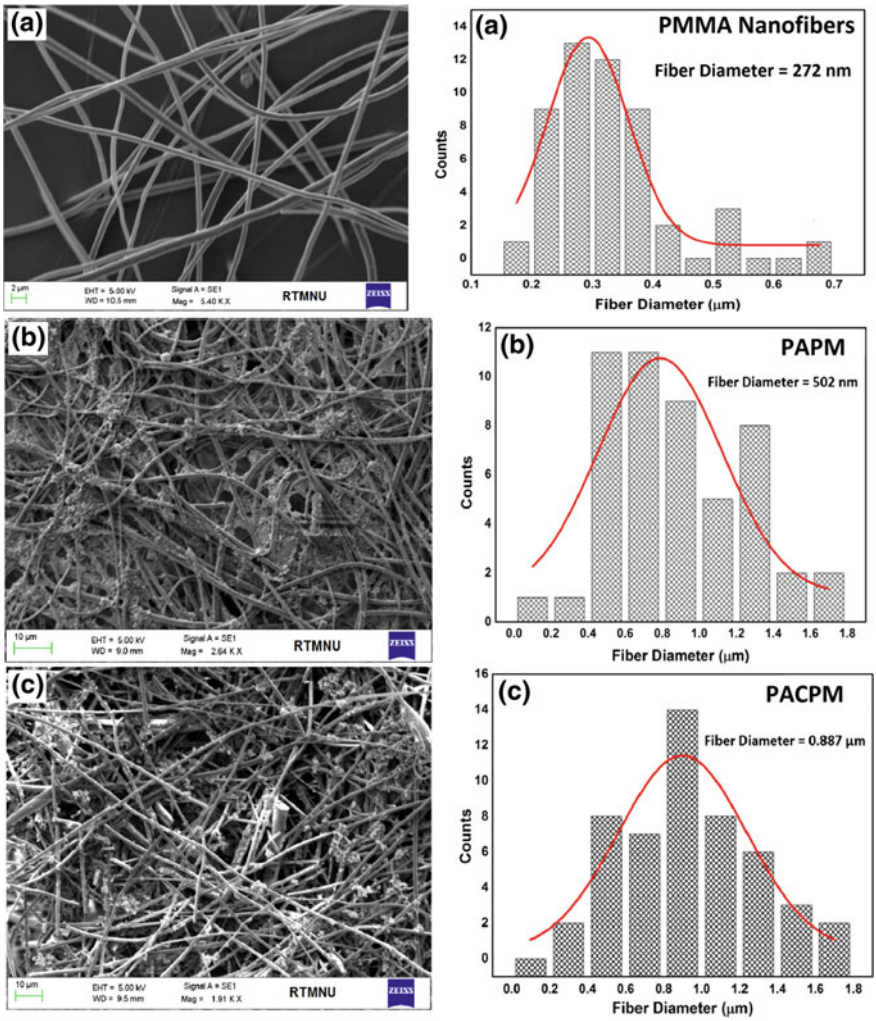

Fig. 1.2 Scanning electron micrographs of **a** PMMA nanofibers, **b** PAPM nanofibers, **c** PACPM composite nanofibers and their respective histograms

nanofibers and its histograms showing distribution of nanofibers diameters. The sample shows the same smooth nature of PMMA nanofibers having nanofiber diameter range of 272 nm, which was increased by the coating of PANI/MWCNTs nanocomposite during in situ polymerization. SEM shows that material coated properly and evenly. Histogram shows that the fiber diameter of PACPM nanofibers is increased to 0.887 μm after coating of PANI/MWCNTs nanocomposite.

1.3.2 FTIR Spectroscopy

FTIR spectra of PAPM and PACPM nanofibers are shown in Fig. 1.3. Yadav et al. reported that, the peaks for PMMA have been recorded at 1731 cm^{-1} for C=O stretching vibrations, 1260–1000 cm^{-1} for C–O (ester bond) stretching vibration, 950–650 cm^{-1} for C–H bending and 3000–2900 cm^{-1} for C–H stretching [15]. In FTIR spectra of PAPM nanofibers, the characteristic peak of PMMA at 1731.62 cm^{-1} (attributed to the –C=O stretching), 1244.64–983.65 cm^{-1} (attributed to ester bonding) and 754.32 cm^{-1}. The peak at 2950.69 cm^{-1} is due to the C–H stretching in PMMA. Peak at 1387.08 cm^{-1} is a characteristic peak of intrinsic PANI indicates C–N stretching. The main peak for PANI observed at 1149.90 and 836.82 cm^{-1} due to the vibration mode of B–NH=Q (benzene-NH-Quinone) or B–NH–B formed in doping reaction. This confirms the fact that PANI has been coated on the surface of PMMA nanofibers. In general, by the addition conducting polymer PANI to the thermoplastic polymer such as PMMA would enhance the optical and mechanical properties of composite nanofibers [15, 18, 21]. The dominant peak at 1149.90 cm^{-1} in the spectrum of both PAPM and PACPM nanofibers can be assigned to the characteristic conductivity peak of polyaniline correspond to "electronic like band" which is considered to be a measure of degree of delocalization of electrons. The introduction of MWCNTs in the polymer resulted in a difference in the intensity of the peaks compared to PAPM nanofibers. This is due to the presence of aniline monomers adsorbed on the surface of MWCNT, resulting in constrained polymerization of PANI on MWCNT confirming the formation of nanocomposite coated PMMA nanofibers. Such constrained motion and adhesion of the polymer chains during polymerization process may restrict the possible modes of vibration in the polymer leading to the difference in intensities in FT-IR spectra compared to PAPM. This interaction may significantly influence the charge transfer process within the polymer as well as

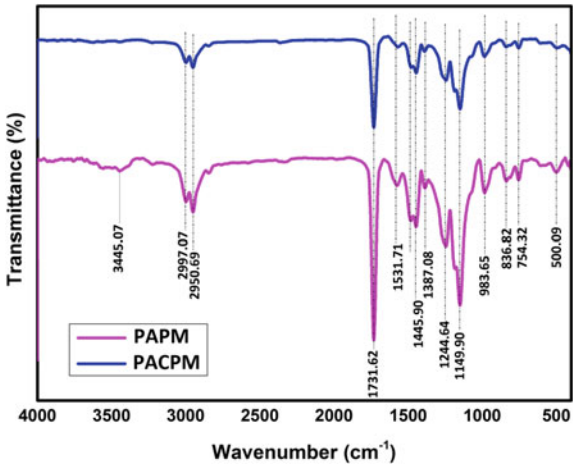

Fig. 1.3 FTIR spectra of PAPM and PACPM nanofibers

between PANI and MWCNT enhancing the conductivity of the composites. PANI has a tendency to strongly interact with the counter material, that is, MWCNTs, PMMA [8, 22, 23].

1.3.3 UV-Vis Spectroscopy

To investigate the interaction of MWCNTs nanomaterials with PANI and PMMA, the UV–visible absorption spectra of synthesized nanofibers were recorded and analyzed. Figure 1.4 shows the UV-Vis Spectrum of PAPM and PACPM nanofibers respectively. For taking UV-Vis spectra, materials were dissolved into the dimethylformamide (DMF) solution and the spectra taken in the range of 200–700 nm. In the spectrum of PAPM and PACPM nanofibers, 279 nm band is assigned to π-π* transition of benzenoid rings, the 328 nm one is assigned to polaron-π* transition, the large absorption band at 617 nm, in the form of a tail is assigned to polaronic bands (i.e. polaron-π* transition and π-polaron transitions) of lower and higher energy mobility and called the free carrier tail [8, 22]. This tail is important for conduction property and becomes more significant. They can be attributed to the polaron transition in the conjugated PANI chains [24]. A very broad tailing that appeared around 617 nm reveals that PANI is highly doped in the synthesized composite nanofibers [23, 25]. Increase in the intensity and red-shifting of the absorbance curve in PACPM nanofibers is due to the addition of MWCNTs into PANI matrix. Interactions between PANI chains and MWCNTs cause easy charge transfer [23].

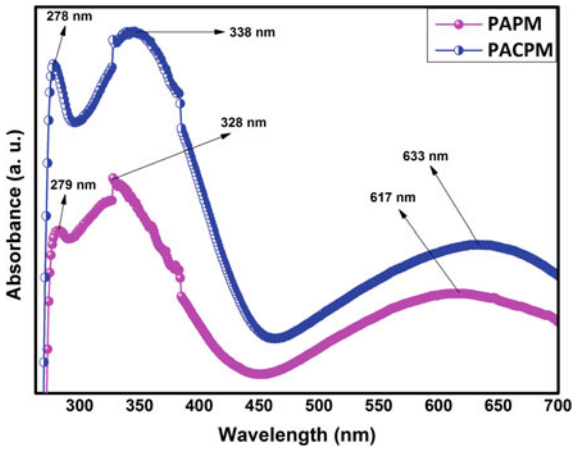

Fig. 1.4 UV-Vis spectra of PAPM and PACPM nanofibers

1.3.4 X-Ray Diffraction

Analysis of X-ray diffraction (XRD) patterns was used to investigate the structure of PAPM and PACPM nanofibers. XRD patterns were obtained in 2θ range between 0° and 90°. Figure 1.5 shows the XRD patterns of PAPM and PACPM nanofibers. XRD patterns of both the samples shows broad peaks at $2\theta = 13.48°$, 33.93° and 42.46°, which are attributed to presence of PMMA. PMMA is known to be an amorphous polymer [21, 26]. In the XRD pattern of PAPM nanofibers, slight sharpening of the main peaks of PANI at $2\theta = 16.89°$, 27.63° and 30.69°, assigned to the periodicity of the repeat unit of the PANI chain and the periodicity parallel to the polymer backbone chain with the broadening of the observed peaks in the PMMA pattern. This amorphous structure is obtained in PAPM nanofibers supporting that PAPM nanofibers formed by an interpenetrating network of PANI and PMMA in which the local ordering of somewhat destructed PANI chains [21, 27]. XRD pattern of PAPM and PACPM nanofibers showed similar peak patterns; therefore, it may be assumed that presence of PANI and MWCNTs did not cause any change in structure of PMMA. The amorphous structure of nanofibers is formed by an interpenetrating network of PANI, MWCNTs and PMMA in which the local ordering of PANI chains is destructed [21]. XRD pattern of PACPM nanofibers owing to the interactions of PANI chains with MWCNTs as indicated by little shifting in their corresponding peaks which mean there is definite chemical interaction between MWCNTs, PANI and PMMA [22].

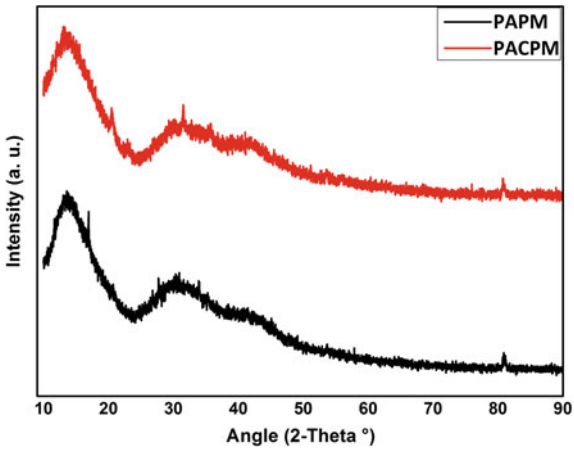

Fig. 1.5 XRD patterns of PAPM and PACPM nanofibers

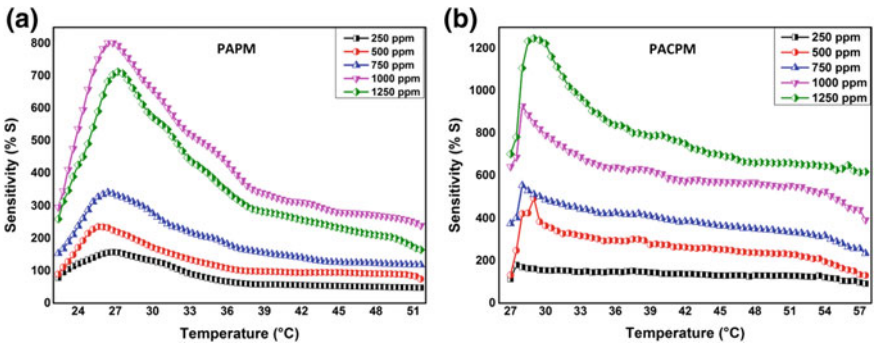

Fig. 1.6 Sensing behaviour of PAPM and PACPM nanofibers

1.3.5 LPG Sensing

The typical changes of the electrical resistance of the composite nanofibers upon interaction with LPG of different concentrations at room temperature are illustrated in Fig. 1.6. PAPM and PACPM nanofibers were tested at varying temperature range from room temperature to higher temperature in the absence and presence of LPG. From Fig. 1.6, it can be seen that the synthesized nanofibers showed a relatively high and fast response towards LPG ranging from 250 to 1250 ppm, which can be soon recovered upon flushing with air [12, 18, 28, 29]. The change in resistance was found in kilo-ohm range. The sensitivity was found to be increased with temperature and reached to the maximum sensitivity at particular temperature and then decreased for higher temperature [18]. LPG is reducing gas [30]. In case of PAPM nanofibers, sensitivity increased up to 26 °C but as the further temperature increased, it gets started to decrease the sensitivity. As the concentration of gas increases, sensitivity factor is also increased at room temperature. In case of PACPM nanofibers, same nature was followed but the sensitivity factor is higher than PAPM, for the range of ppms. It is generally proposed that nanostructured sensing materials exhibit a higher surface-to-volume ratio, thus provide more sites for adsorption of analyte molecules and achieve a higher sensitivity than their thin film counterparts [12, 18].

The electrical response of the PACPM nanofibers to LPG forms conducting paths inside the MWCNT/polymer composites due to quantum mechanical tunneling effects, where the distance between the conducting sticks is such that electron hopping can occur. The contact resistance between MWCNTs increases owing to an increase in distance between adjacent nanotubes. Swelling of the polymer matrix due to absorption of LPG may also increase the volume and thus increase the distance between nanotubes, thereby increasing the contact resistance. The extent of swelling, and hence the electrical response, depends on the solubility of the polymer in the solvent. Alternation of electronic properties of the semiconductor CNT surface occurs by charge transfer induced by adsorption of polar organic molecules. The adsorption of such molecules is due to the polar nature of surface as well as that of the solvent molecule [31].

Carbon nanotubes are a very sensitive material because they can easily interact with many gases and change their conductivity in the presence of several analytes at room temperature, even if these analytes have different chemical behaviour [32]. Because of the arrangement of the atoms on the surface of the MWCNTs and their high area/volume ratio, adsorption processes are highly favoured, which increases their sensitivity to the surrounding atmosphere. PANI can act as the sensing layer because it is more selective (although selectivity is not complete) than the raw MWCNTs, which then act as the transducer part. A change in the electrical conductivity of the MWCNTs caused by the effect of the analyte on their surface may have two consequences: they may promote a charge transfer from the analyte to the nanotubes, or the analyte may act as a scattering potential. The charge transfer increases the conductivity when the analyte adsorbed is an electron attractor (hole donation). If the analyte is an electron donor, the number of holes on the nanotubes will decrease, which leads to a decrease in the electrical conductivity [1]. LPG is electron donor, hence the resistance of PACPM nanofibers was increased when it exposed to LPG.

The sensing mechanism is complex and the possible cross interaction between the PANI and MWCNTs is not yet fully understood. It is known that during polymerization, emeraldine salt is formed onto the surface of MWCNTs, making the PANI a p-type semiconductor with N^+-H adsorption sites. The MWCNTs are also p-type semiconductors with holes as major charge carriers. A simplistic representation of the sensor calls for the PCPM nanofibers to be considered as two resistances in parallel. The current will essentially flow through the lowest resistance component. For PANI, the resistance change will be modulated by the protonation-deprotonation brought by LPG. As LPG molecule adsorbs onto or is absorbed into the polymer, LPG (Which is simply a mixture of butane, propane, butylene and propylene) molecules withdraw protons from N^+-H sites. This deprotonation process reduces PANI from the emeraldine salt state to the emeraldine base state, leading to reduced hole density in the PANI and thus an increased electrical resistance. When the sensor is purged with air, the process is reversed and the initial doping level and electrical resistance are restored. In addition to the two-resistance in parallel model, PACPM nanofibers can be considered as one p-type semiconductor network. The interaction between PANI and MWCNTs may increase the p-electron delocalization which leads to the higher charge transfer between PANI and MWCNT. Detailed investigations of the sensing mechanism are warranted [33].

The main advantage of nanostructured materials is considered to be related with the enlargement of active surface area for adsorption. According to adsorption law, the adsorption ability of an adsorbent is greatly determined by its surface area [34]. Addition of MWCNTs into the polymeric matrix of PACPM nanofibers increases the surface area to volume ratio, which provides more active sites for adsorption of gas molecules leads to a larger response because gas molecules can penetrate hybrids rapidly and allow more opportunities for reaction. Moreover, they enhance intrinsic charge transport due to high carrier mobility. MWCNT plays important roles in improving the charge transport because MWCNT has extremely high mobility compared to PANI. Thus, the addition of MWCNT in the polymer matrix created an easier path for charge transport between electrodes, even in small amount of

LPG [35]. From Fig. 1.6 it can be seen that, the sensitivity of PAPM and PACPM nanofibers is almost same i.e. 154.94 and 177.35 respectively for 250 ppm at room temperature. LPG is a mixture of hydrocarbons. The molecules of hydrocarbons are nonpolar because the atoms in the molecules have same electronegativity. Hence, alteration of electronic properties of semiconductor couldn't be occurring. This very less change in sensitivity observed may be due to the less amount of LPG get absorbed on the PACPM nanofibers. Very less amount of LPG couldn't generate more carriers and form sufficient conducting paths for the charge transport due to carrier mobility inside PACPM nanofibers by which the electron hopping occur. As the amount of gas increases, more conducting paths get created and hence PACPM nanofibers sense more LPG and shows good sensitivity at room temperature [31].

Figure 1.7 shows the Sensitivity versus concentration plot for PAPM and PACPM nanofibers. From the graph it can be seen that as the ppms of LPG increases, the sensitivity factor of PAPM and PACPM nanofiber increases. But the sensitivity of PACPM nanofibers is higher than PAPM nanofibers [36].

Figure 1.8a, b shows the dynamic variation of the response of the PAPM and PACPM nanofibers sensor with time upon exposure to 250–1250 ppm of LPG at room temperature. The figure revealed that the initially the response of sensor nanofibers increase with increasing the concentration of LPG. At 1250 ppm, PAPM and PACPM nanofibers sensor showed the maximum response of 6.83 and 11.85 respectively. Such a higher value of response is believed to be due to the sensitivity of the semiconductor sensors mainly determined by the interactions between the target gas and the surface of the sensor. So, it is obvious that for the materials of greater surface area, the interactions between the adsorbed gases and the sensor surface are significant [6, 37]. Depending on LPG concentration, the response time (defined as the time to reach 90% of the total resistance change) of PAPM and PACPM nanofibers sensors to LPG exposure was on the order of a few seconds, while recovery time ranged from several seconds to a few minutes for the sensor to recover to its original resistance [33].

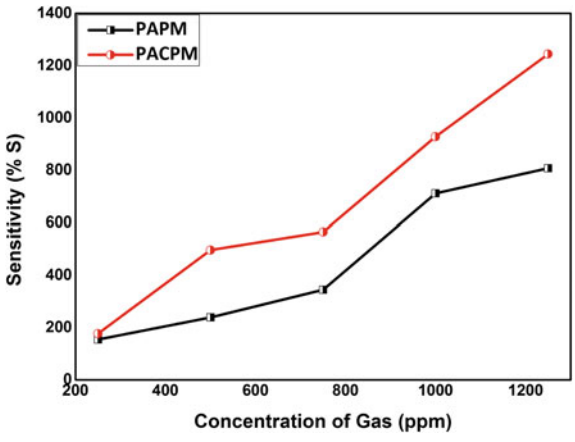

Fig. 1.7 Sensitivity versus concentration for PAPM and PACPM nanofibers

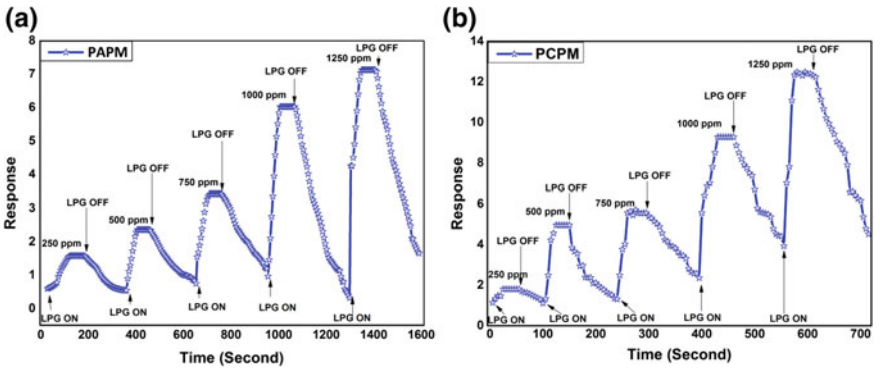

Fig. 1.8 Sensing response and reversibility for **a** PAPM and **b** PACPM Nanofibers

From graphs, it can be seen that the composite nanofibers showed a relatively high and fast response towards LPG ranging from 250 to 1250 ppm as the sample have porous fibrous structure in which the gas analytes accommodate easily. The response time of PAPM and PACPM was found to be 8 s and 13 s respectively for 1250 ppm with maximum response of 6.83 and 11.85 respectively. But the response time for PAPM and PACPM for the range 250–1000 ppm is almost same. Samples showed good reproducible resistance change for a number of cycles [38].

The average response and recovery times for PAPM and PACPM nanofibers are faster than the response time of the PAPM nanofiber [18]. From the same graph, it is found that for higher concentrations of LPG, the recovery time was long. This may probably be due to the heavier nature of LPG and the reaction products are not leaving from the interface immediately after the reaction [6, 18]. The responses with good recovery can be a great advantage for the potential application of the PAPM and PACPM nanofibers [8, 18].

Figure 1.9 shows the stability curve of PAPM and PACPM nanofibers. The sensitivity of these samples was studied for 10 days for 250 ppm of LPG at room temperature. It has been observed that the sensitivity value of the samples was found to be very little change when tested for 10 days indicating the good stability of these samples towards 250 ppm of LPG at room temperature (27 °C). Hence, the synthesized composite nanofibers of PAPM and PACPM nanofibers are the very stable sensing materials for LPG.

1.4 Conclusions

PAPM and PACPM nanofibers were prepared by using electrospinning technique and an in-Situ chemical oxidative polymerization method. SEM micrograph of PMMA, PAPM and PACPM nanofibers with their respective histogram shows that the average diameter of the fibers was increased by the coating of PANI and PANI/MWCNT

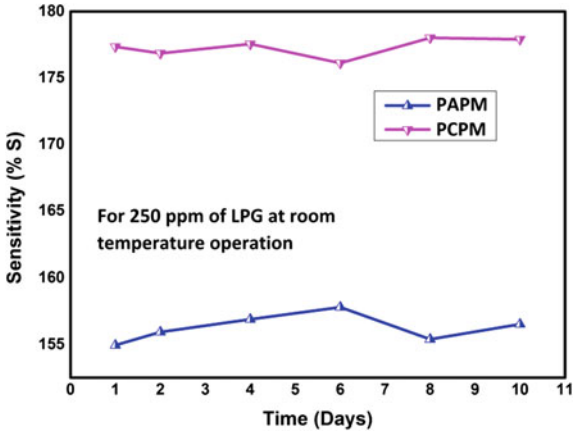

Fig. 1.9 Stability curve for PAPM and PACPM nanofibers

nanocomposites. UV-Vis, FT-IR and XRD analyses confirmed the formation of PANI and its interaction with MWCNTs. Sensitivity study shows that materials under investigation are found to be highly sensitive for LPG near to room temperature. The dynamic variation of the response of PAPM and PACPM nanofibers shows sensor upon exposure to 250–1250 ppm of LPG at room temperature revealed that initially the response of sensor nanofibers increase with increasing the concentration of LPG. From response curves of the nanofibers it was observed that for repeated exposure and removal of LPG (250–1250 ppm), PAPM and PACPM nanofibers showed good reproducible resistance change for a number of cycles. Stability plot explains that, the synthesized nanofibers of PAPM and PACPM are the very stable sensing materials for LPG.

Acknowledgements The authors are thankful to UGC (India) for providing financial assistance and BSR Fellowship to carry out this research work File No. F.39-540/2010(SR) and F.4-1/2006(BSR)/7-154/2007(BSR).

References

1. G. Jimenez-Cadena, J. Riu, F. Xavier Rius, Gas sensors based on nanostructured materials. RSC Analyst **132**, 1083–1099 (2007)
2. K. An, S. Jeong, H. Hwang, Y. Lee, Enhanced sensitivity of gas sensors incorporating single walled carbon nanotubes-polypyrol nanocomposites. Adv. Mat **16**, 1005–1009 (2004)
3. S. Pandey, Highly sensitive and selective chemiresistor gas/vapor sensors based on polyaniline nanocomposite: a comprehensive review. J. Sci. Adv. Mater. Devices **1**, 431–453 (2016)
4. R. Singh, N. Kohli, M. Singh, O. Singh, Ethanol and LPG sensing characteristics of SnO_2 activated Cr_2O_3 thick film sensor. Bull. Mater. Sci. **33**, 575–579 (2010)
5. D. Dhawale, D. Dubal, A. More, T. Gujar, C. Lokhande, Room temperature liquefied petroleum gas (LPG) sensor. Sens. Actuators B **147**, 488–494 (2010)

6. D. Dhawale, D. Dubal, V. Jamadade, R.R. Salunkhe, S. Joshi, C. Lokhande, Room temperature LPG sensor based on n-CdS/p-polyaniline heterojunction. Sens Actuators B **145**, 205–210 (2010)
7. I. Fratoddia, I. Vendittia, C. Camettib, M. Russo, Chemiresistive polyaniline-based gas sensors: a mini review. Sens Actuators B **220**, 534–548 (2015)
8. S. Abdulla, T. Mathew, B. Pullithadathil, Highly sensitive, room temperature gas sensor based on polyaniline-multiwalled carbon nanotubes (PANI/MWCNTs) nanocomposite for trace-level ammonia detection. Sens Actuators B **221**, 1523–1534 (2015)
9. S. Virji, J. Huang, R. Kaner, B. Weiller, Polyaniline nanofiber gas sensors: examination of response mechanisms. Nano Lett. **4**, 491–496 (2004)
10. R. Gangopadhyay, A. De, Conducting polymer nanocomposites: a brief overview. Chem. Mater. **12**, 608–622 (2000)
11. S. Ji, Y. Li, M. Yang, Gas sensing properties of a composite composed of electrospun poly(methyl methacrylate) nanofibers and in situ polymerized polyaniline. Sens. Actuators B **133**, 644–649 (2008)
12. M. Shin, Y. Kim, S. Kim, S. Kim, H. Lee, G. Spinks, S. Kim, Enhanced conductivity of aligned PANi/PEO/MWNT nanofibers by electrospinning. Sens. Actuators B **134**, 122–126 (2008)
13. F. Jian, N. Tao, L. Tong, W. Gai, Applications of electrospun nanofibers. Chin. Sci. Bull. **53**, 2265–2286 (2008)
14. B. Aronggaowa, M. Kawasaki, T. Shimomura, Thin, transparent conductive films fabricated from conducting polymer nanofibers. Polym. J. **5**, 819–823 (2013)
15. J.B. Yadav, B. Patil, R. Puri, V. Puri, Studies on spin coated PANI/PMMA composite thin film: effect of post-deposition heating. Appl. Surf. Sci. **255**, 2825–2829 (2008)
16. T. Zhang, S. Mubeen, N. Myung, M. Deshusses, Recent progress in carbon nanotube-based gas sensors. Nanotechnology **19**, 332001–332014 (2008)
17. R. Sabzi, K. Rezapour, N. Samadi, Polyaniline–multi-wall-carbon nanotube nanocomposites as a dopamine sensor. J. Serb. Chem. Soc. **75**, 537–549 (2010)
18. P. Patil, R. Anwane, S. Kondawar, Development of electrospun polyaniline/ZnO composite nanofibers for LPG sensing. Procedia Mater. Sci. **10**, 195–204 (2015)
19. J. Stejskal, R. Gilbert, Polyaniline preparation of a conducting polymer. Pure Appl. Chem. **74**, 857–867 (2002)
20. I. Sapurina, J. Stejskal, The mechanism of the oxidative polymerization of aniline and the formation of supramolecular polyaniline structures: polymer international. Polym. Int. **57**, 1295–1325 (2008)
21. A. Fattoum, F. Gmati, N. Bohli, A. Arous, A. Mohamed, Effects of the matrix molecular weight on conductivity and dielectric relaxation in plasticized polyaniline/polymethylmethacrylathe blends. J. Phys. D: Appl. Phys. **41**, 095407–095416 (2008)
22. V. Gautam, A. Srivastava, K. Singh, V. Yadav, The mechanism of the oxidative polymerization of aniline and the formation of supramolecular polyaniline structures. Polym. Compos. 1–11 (2015)
23. L. Shi, R. Liang, J. Qiu, Controllable deposition of platinum nanoparticles on polyaniline-functionalized carbon nanotubes. J. Mater. Chem. **22**, 17196–17203 (2012)
24. M. Chougule, S. Sen, V. Patil, Facile and efficient route for preparation of polypyrrole-ZnO nanocomposites: microstructural, optical, and charge transport properties. J. Appl. Polym. Sci. **125**, E541–E547 (2012)
25. A. Mostafaei, A. Zolriasatein, Synthesis and characterization of conducting polyaniline nanocomposites containing ZnO nanorods. Prog. Nat. Sci. Mater. Int. **22**, 273–280 (2012)
26. N. El-Zaher, M. Melegy, O. Guirguis, Thermal and structural analyses of PMMA/TiO2 nanoparticles composites. Nat. Sci. **6**, 859–870 (2014)
27. Q. Yao, J. Chang, L. Chen, Enhanced thermoelectric properties of CNT/PANI composite nanofibers by highly orienting the arrangement of polymer chains. J. Mater. Chem. **22**, 17612–17618 (2012)
28. S. Kondawar, P. Patil, S. Agrawal, Chemical vapour sensing properties of electrospun nanofibers of polyaniline/ ZnO nanocomposites. Adv. Mat. Lett. **5**, 389–395 (2014)

29. S. Kondawar, S. Agrawal, S. Nimkar, H. Sharma, P. Patil, Conductive polyaniline-tin oxide nanocomposites for ammonia sensor. Adv. Mat. Lett. **3**, 393–398 (2012)
30. F. Tudorache, N. Rezlescu, N. Tudorache, A. Catargiu, M. Grigoras, Polyaniline and polythiophene-based gas sensors. Optoelectron. Adv. Mater. Rapid Commun. **3**, 379–382 (2009)
31. B. Philip, J. Abraham, A. Chandrasekhar, V. Varadan, Carbon nanotube/PMMA composite thin films for gas-sensing applications. Smart Mater. Struct. **12**, 935–939, 2003
32. H. Guerin, H. Poche, R. Pohle, E. Buitrago, M. Badía, J. Dijon, A. Ionescu, Carbon nanotube gas sensor array for multiplex analyte discrimination. Sens. Actuators B **207**, 833–842 (2015)
33. T. Zhang, B. Megan, M. Nix, B. Yoo, M. Deshusses, N. Myung, Electrochemically functionalized single-walled carbon nanotube gas sensor. Electroanalysis **18**, 1153–1158 (2006)
34. K. Yan, Y. Toku, Y. Ju, Highly sensitive hydrogen sensor based on a new suspended structure of cross-stacked multiwall carbon nanotube sheet. Int. J. Hydrogen Energy **055**, 1–9 (2019)
35. S. Park, C. Park, H. Yoon, Chemo-Electrical Gas Sensors Based on Conducting Polymer Hybrids. Polymers **9**, 155 (2017)
36. H. Tai, Y. Jiang, G. Xie, J. Yu, X. Chen, Z. Ying, Influence of polymerization temperature on NH3 response of PANI/TiO2 thin film gas sensor. Sens. Actuators B **129**, 319–326 (2008)
37. S. Patil, M. Chougule, S. Sen, V. Patil, Measurements on room temperature gas sensing properties of CSA doped polyaniline–ZnO nanocomposites. Measurement **45**, 243–249 (2012)
38. N. Deshpande, Y. Gudage, R. Sharma, J. Vyas, J. Kim, Y. Lee, Studies on tin oxide-intercalated polyaniline nanocomposite for ammonia gas sensing applications. Sens. Actuators B **138**, 76–84 (2009)